






Design and evaluation of low-power switching power supplies using a zero-voltage boost converter with a snubber circuit

 Teerawut Savangboon¹,  Arckarakit Chaithanakulwat^{2*},  Nuttee Thungsuk³,  Thaweesak Tanaram⁴,  Papol Sardyoung⁵

^{1,2,3}Department of Electrical Engineering, Faculty of Science and Technology, Dhonburi Rajabhat University, Samut Prakan 10540, Thailand; teerawut.s@dru.ac.th (T.S.) akharakit.c@dru.ac.th (A.C.) nuttee.t@dru.ac.th (N.T.)

⁴Department of Power Electrical Engineering Technology, Faculty of Industrial Technology, Pibulsongkram Rajabhat University, 65000, Thailand; tummut2001@yahoo.com (T.T.)

⁵Department of Electrical Technology Industrial, Faculty of Industrial Technology, Thepsatri Rajabhat University, 15000, Thailand; papol_s@hotmail.com (P.S.).

Abstract: Switching power supplies are widely popular because they are sufficiently small to fit all types of electrical appliances. Adjusting the pulse width modulation (PWM) of the switching power supply under high-frequency conditions often causes switching losses. PWM also causes electromagnetic interference (EMI) under high-frequency switching conditions. These problems can be solved using soft switching, which can adequately reduce the losses under switching conditions and EMI-induced noise. Therefore, this study describes the design and evaluation of a zero-voltage boost converter with a snubber circuit for a low-power switching power supply, which reduces the performance loss of the switching power supply under high-frequency conditions. This study was divided into two main parts. The first part focuses on the use of TMS320F28377S microcontrollers, which are outstanding in their precise control and can simulate switching within the MATLAB/Simulink program environment, and studies the switching behavior of boost converters in detail, making the switching power supply high performance and reliable. The second part focuses on evaluating the performance of the boost converter under different conditions, consisting of a state stimulated by the snubber circuit and a non-stimulated state by the snubber circuit. However, the evaluation showed that the boost converter in the space activated by the snubber circuit had an 85.16% increase in performance, which was 6.75% higher than that in the no-stimulation state with the snubber circuit. Similarly, the switching power supply can control and maintain a constant voltage, and this effect is satisfactory and reliable.

Keywords: Boost converter, Microcontroller, Snubbers, Zero current, Zero voltage.

1. Introduction

DC-DC converter-switching power supplies are important sought-after mechanisms for various renewable energy sources. This DC-DC converter mechanism, in which fast response to changes and easy control are desired, must increase the switching frequency to achieve high power. The device used in the converter and PWM should be small because of its high power and reduced noise level owing to its operation. This high switching frequency often results in high switching losses and electromagnetic interference (EMI) [1]. Therefore, their performance and efficiency are low. Soft-switching techniques have been used to overcome these side effects [2]. Soft switching is typically responsible for eliminating or reducing the switching losses and EMI noise. Therefore, the circuit developed and used to achieve soft switching is called a snubber circuit. In traditional DC-DC converters, the operation of the boost switch must first provide a voltage drop to zero, so that the PWM signal can be controlled to operate as

a zero-voltage transition. Therefore, this control condition uses a snubber circuit to control the operation of the boost switch when turned off. Thus, the boost switch is activated with a zero-voltage transition without loss. The snubber switch turns on with zero-current switching using the same valve, and the boost diode turns off, but not completely [3]. Similarly, if the snubber switch is off, it turns off under heavy switching conditions. In addition, if the circuit operates at low loads, its operation is inefficient. However, various studies have investigated these problems by using common zero-voltage transition techniques.

The method of reducing the current flow through the zero-boost switch while turning off the traditional boost converter is typically used to change the current to zero with a circuit. In this state, the boost-switch control signal is zero when the current is zero. Thus, the boost switch is switched off with a zero voltage change and no loss [4]. Additionally, the boost diode can be turned on under soft switching. The snubber switch and boost diode were turned off using hard-switching. In addition, the boost diode exhibited high reverse recovery loss. A study of these problems was presented to solve the zero-voltage transition technique by having the boost switch turn on with zero-current switching and turn off with zero-voltage transition [5]. Therefore, the switching power loss is reduced compared with that of conventional zero-voltage transition converters. Studies have shown that certain types of converters can reduce the switching losses. The current stress is high, and the overall efficiency is reduced owing to loss of circulation. Voltage stress also occurred at the snubber switches [6]. However, there are many other types of devices that support the flow of current through the boost switch in the circuit as well as devices that are used to support the flow of current through many snubber switches. However, the snubber circuit design process is difficult and complex. According to the literature on snubber circuitless converters, even with soft switching, boost switches are subjected to stress from large amounts of current and voltage. Therefore, soft switching by leaps occurs only in a small fraction of power consumption.

According to relevant literature, booster converter circuits are often used in a variety of applications, including modifying the power factor of current LED lamps, voltage regulation, and renewable energy systems [7]. The demand for high power density has led to an increase in high-efficiency DC-DC power generation over the past few decades. Switching converters are a good option for achieving these goals, as they can support power levels of up to several kilowatts while still providing a high efficiency. Furthermore, switching converters, such as aerospace converters, are important, particularly in areas that require low weight. However, the main disadvantage of switching converters is their high stress level. Consequently, the voltage and current of power semiconductor devices and inductive components are overheated because of switching. Zero-voltage and zero-current switching are popular soft switching methods. This method minimizes the voltage and stress of the current in the inductor [8]. Therefore, the speed of change must also be reduced. Therefore, the inverted operation was turned off before the independent wheel diode began to operate. However, resonant snubber circuits have been used in some studies to help the boost switch turn on at zero voltage. However, there are now a variety of zero-voltage and zero-current transition techniques, and many specialized ICs have been produced [9].

Boost converter circuits are highly efficient, and a high step-up voltage gain is widely used in a wide range of applications such as offline AC to DC power supplies and solar power systems. However, a typical converter boost circuit may suffer from high voltage surges through the main power switch and losses in the switching power supplies of the DC-DC converter [10]. This is especially true in applications that require high voltage conversion ratios. In recent years, many researchers have focused on soft-switching techniques to reduce the voltage stress on boost switches and to reduce losses. Zero-voltage and zero-current transitions are the most popular soft-switching techniques for inverter-boost circuits [11]. This can be used to achieve a zero-voltage transition by adding a snubber circuit to the main power switch. The most common solution is to increase the number of snubber circuits, inductors, and capacitors in the circuit snubber to achieve soft-switching. In addition, boost converter operation was configured [12]-[13]. Consequently, the ratio of the maximum output voltage was reduced to 1:4

of the input voltage to achieve a higher output voltage. This method involves the addition of a special switch and voltage multiplier to a common boost converter, called a booster converter, with a voltage multiplier cell.

However, the voltage stress of the main power switch and diode in the voltage multiplier cell is high, particularly in the case of a high output voltage. Modern power semiconductor switches, including metal oxide-semiconductor field-effect transistors (MOSFETs) and insulated gate bipolar transistors (IGBTs), are widely used in power electronics systems, such as switch-mode power supplies, DC-AC converters, motor drivers, and electric vehicles [14]. Currently, power MOSFETs are the most widely used and reliable switches in power electronic systems. The control of the turn-on and turn-off of power MOSFETs is reliable, so it is used to control output power waveforms in applications such as motor drivers and DC-AC inverters. However, as mentioned in the previous subsection, power MOSFETs in boost converters are subjected to high-voltage stress and high turn-on losses. Moreover, a common solution with the addition of a passive snubber circuit results in a greater energy loss with the resistor. Snubber circuits can be used as active clamping circuits to solve the problem of voltage surges in main power switches, but special voltage clamping switches and drive circuits complicate this solution. Similarly, turning off an inductive boost switch is theoretically feasible because it can provide an increase in voltage to turn off the MOSFET and bring the power to zero. However, some practical problems may arise, such as power consumption of the control logic and conduction at high frequencies.

This study aims to design and evaluate a zero-voltage boost converter with a snubber circuit for low-power switching power supplies to reduce losses and increase the efficiency of switching power supplies under high-frequency conditions. The objectives of this study are as follows: (1) Design and evaluation of a zero-voltage boost converter with a snubber circuit that uses a TMS320F28377S microcontroller to control the switching of power electronics. (2) Using a TMS320F28377S microcontroller, the switching of the device was simulated in the MATLAB/Simulink program environment to study the switching behavior of the boost converter. (3) The evaluation of the performance of this mechanism has two different operating conditions: operating and non-operating conditions of the snubber circuit. The remainder of this article is structured as follows: the second part of the proposed methodology, the third part of the research methodology, the fourth part of the results and discussion, and the fifth part of the conclusion.

2. Proposed Methodology

This study aims to investigate and develop a zero-voltage transition technique for a booster converter circuit with the excitation of a snubber circuit. The zero-voltage transition technique has been widely used in literature. Compared with the traditional fixed-frequency switching method, this newly designed and developed zero-voltage transition technique can reduce the EMI problems. In addition, zero-voltage transitions and various soft-switching techniques have been investigated. Among them, the zero-voltage switching technique has attracted much attention because of its advantages, such as the possibility of turning on a power switch with zero voltage and reducing the voltage surge. Many researchers have used resonant switches to achieve soft switching in converters. However, the complexity of configuring different devices in circuits, waveforms, and voltage currents has become an obstacle in the development of resonant switches. Furthermore, it has been demonstrated that the zero-voltage transition technique for boost converters requires complex circuitry and control algorithms. However, the amount of energy transferred from the element and the switching frequency depend on the load conditions. However, the experimental results showed that the resonant current and voltage waveforms were successful, with the help of qualitative and quantitative analyses in the laboratory. Soft-switching characteristics and design rules were evaluated. It has also been successful in predicting large-signal behavior and in conducting theoretical analysis using a zero-voltage transition strategy designed and developed for boost converters. Similarly, snubber circuits are used to eliminate voltage and current surges in switching devices and provide a pathway for the discharge of inductive energy from switching devices, thereby causing a voltage surge rate and protecting the switch from high-

voltage stress. In addition, the power loss of the resistors in the snubber circuits and the effects of the snubber circuits are discussed. It has also been shown to reduce the voltage stress in the boost switch and the power loss of the snubber circuits. This verifies that the goal of the stimulation with the snubber circuit can be achieved.

The diagram in Fig. 1 shows a boost converter with a zero-voltage transition operating with snubber circuitry. This snubber circuit is intended to allow inductive current to flow when the switch encounters an electromagnetic force (EMF) due to the sudden turn-off of the switch. The function of the snubber circuit starts only when the switch is turned on and does not involve the turn-off of the snubber circuit, which can be customized to protect against voltage and current surges and does not need to absorb all energy [15]. However, because of the energy-absorption time, it can be designed to be longer than the turn-off time. The energy stored in the inductive converter was then transferred to the circuit capacitor. snubber and eventually dispersed with the resistor. However, as shown in Fig. 1, the proposed boost converter comprises a suppressor circuit with a snubber switching device, two resonant inductors, two resonant capacitors, and two snubber diodes. The designed boost converter begins with the operation of the boost switch [16]. It turns on with zero-voltage switching and off with zero-voltage switching. The snubber switch was turned on with zero-current switching, and closed with zero-voltage switching. The boost diode turns on with zero-voltage switching and turns off with zero-current switching, which does not affect the voltage or current stress of the boost switch or diode [17]. This voltage stress does not occur on the snubber switches and diodes if these switching devices are turned on and off under soft switching. However, the proposed converter can operate under the application of a required load without consuming a significant amount of energy. Therefore, the transient interval that occurs has a very small total in the switching cycle, thus causing switch S_b to open in a zero-voltage condition. In this research, the Opt for MOSFET-type semiconductor devices is the primary switch for boost converter switching devices. The reason for using this MOSFET is that capacitor power can only be recovered using the zero-voltage switching technique. An insulated gate two-pole transistor (IGBT) was chosen as the snubber switch because the zero-voltage transition can protect the tail current when it is closed.

Figure 1 shows that the main circuit of the converter consists of V_i , which is the input voltage supply that converts AC-DC to a circuit. bridge rectifier. S_b is the boost switch in the boost circuit, L_r is the main inductor in the boost circuit, and C_f is the capacitor used to filter the output ripper, D_f It is the boost diode in the boost circuit, and C_s is the capacitor in the buffer circuit linked to the boost converter. As for the snubber circuit section, it consists of D_r , D_s as snubber diodes, C_r , C_s , and L_r as resonance capacitors and resonant inductors respectively, with S_n as the control switch in the snubber circuit. Fig. 1 If circuit theory is used to analyze the characteristics of the circuit in the overall configuration, a constant input voltage (V_i) is obtained. Capacitor (C_f) must be sufficiently large to maintain a constant output voltage. Similarly, the inductor (L_r) must be large enough to filter and maintain the required input current ripples, and more importantly, the inductor (L_r) must be much larger than L_r . However, let us assume that all semiconductor devices are appropriate, and that the recovery times of D_r and D_s , except for D_r , which is ignored, ignore the voltage drop.

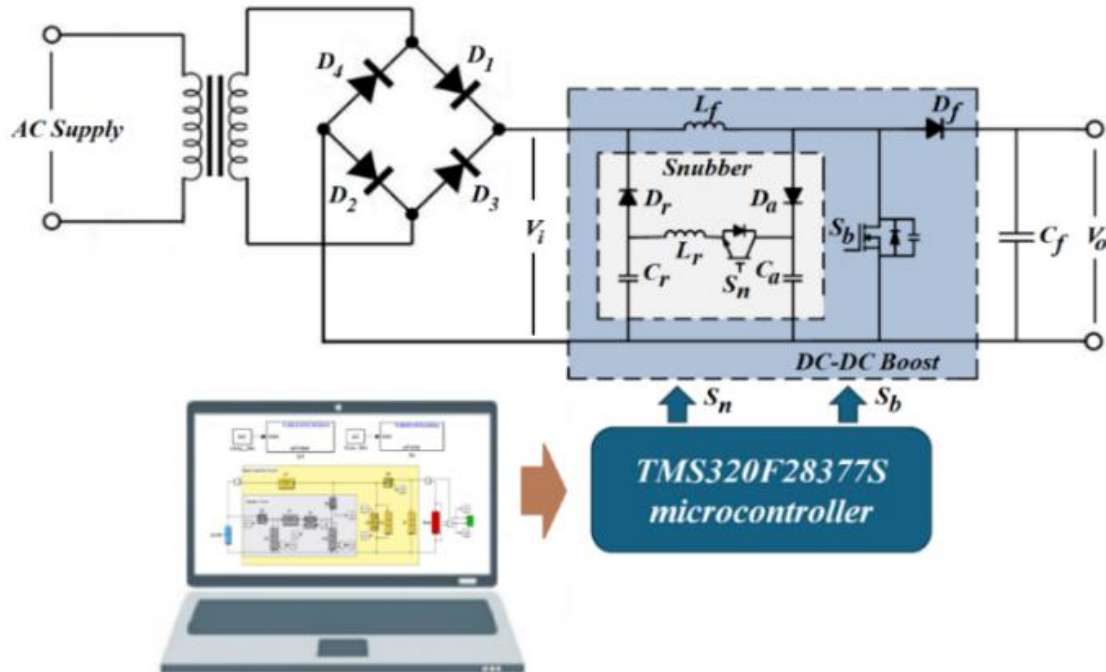


Figure 1.
Diagram of a zero-voltage boost converter with a snubbers circuit.

3. Research Methodology

The following sections describe the definitions and principles involved, as well as the operational procedures proposed in this study, which are described in detail.

3.1. Analysis of Operation

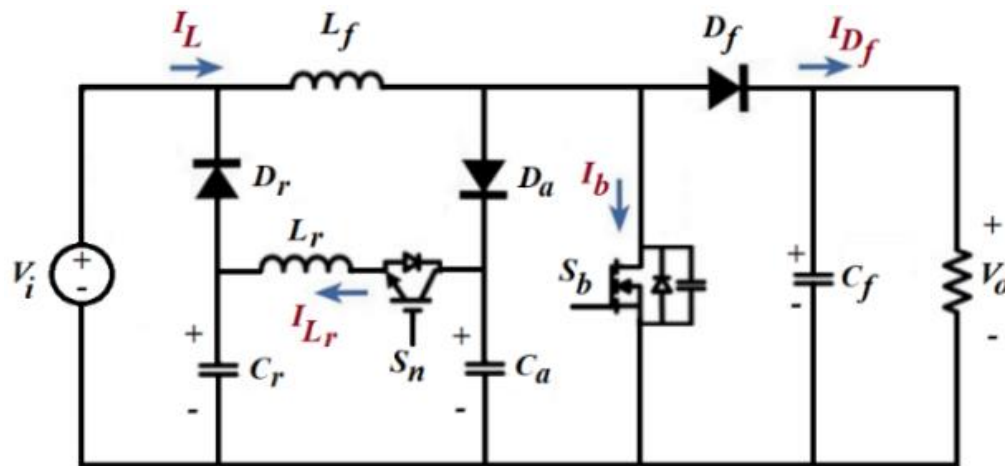


Figure 2.
Equivalent circuit of the boost converter and snubber.

Figure 2 Equivalent circuits of boost converters and snubber circuits designed and used for performance evaluation based on the configuration defined in. Fig. 3. shows the operating status of the

boost converter and the snubber in one cycle. This equivalent circuit can convert the operating state into ten states, as shown in Figure 3 (a) – (j).

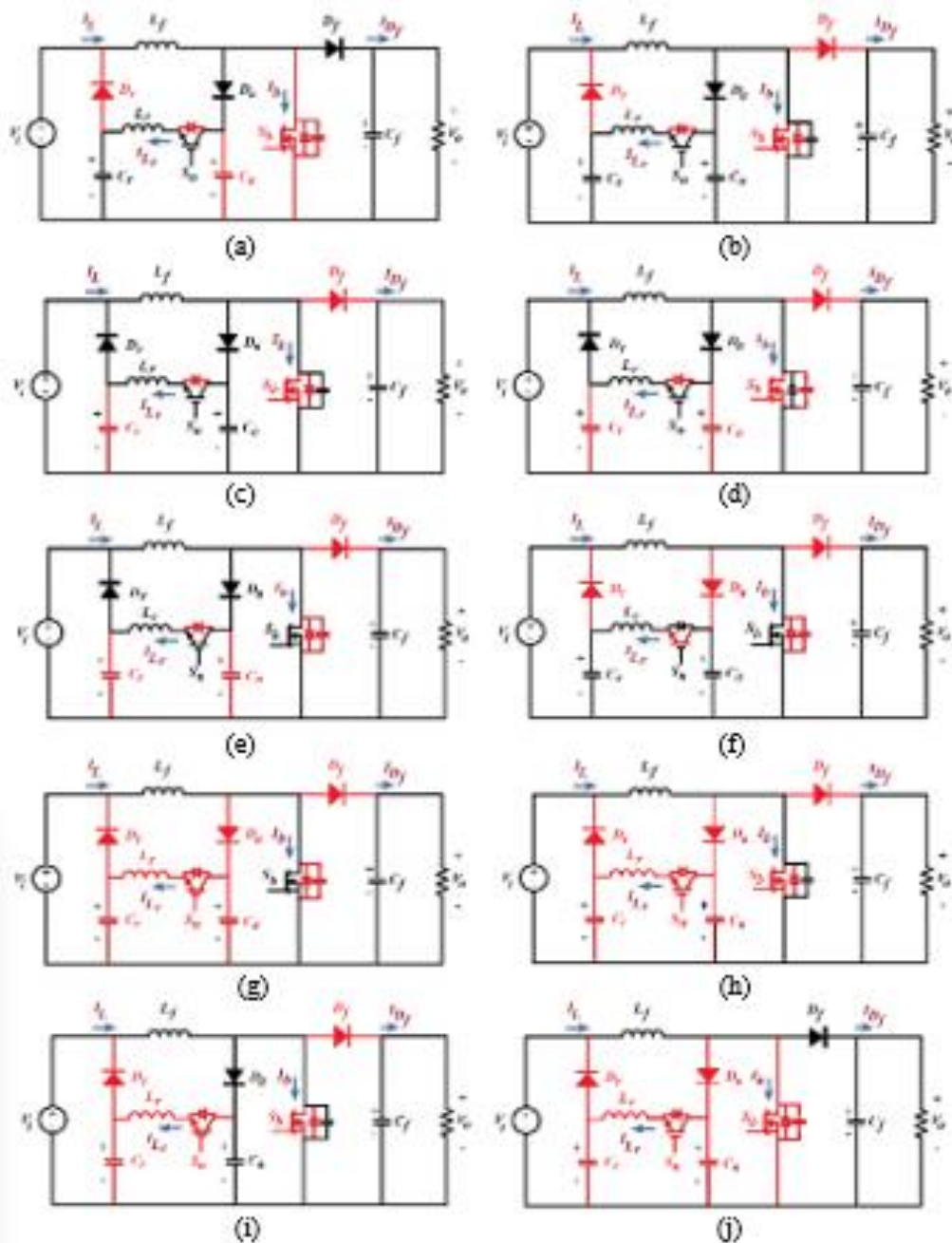


Figure 3.
Schematics of the operation stages of the boost converter and snubber.

Figure 3 (a) Stage 1: $t_0 < t < t_1$. Boost switches S_b and S_n are in a normal turn-off state as the starting state. In this starting state, I_L flows to the output through D_f according to the turn-off state of a typical boost converter. This state yielded the following attributes: $t = t_0$, $I_b = 0$, $I_{Df} = I_L$, $I_r = I_n = 0$, $V_{C_a} = V_0$, and $V_c = 0$. However, the PWM signal is applied to control the switch S_b at $t = t_0$, which is the initial

interval. Similarly, I_{Df} is reduced, and C_r is simultaneously charged at the same time. $I_{Lr}(t)$ and the voltage of $V_{Cr}(t)$ can be expressed as follows:

$$t_o = \frac{1}{\omega_1} \cos^{-1} \left(\frac{V_{Ca} - V_o}{-V_o} \right) \quad (1)$$

$$V_{Cr}(t) = -V_o \cos(\omega_1 t) + V_o \quad (2)$$

$$I_{Lr}(t) = \frac{V_o}{Z_1} \sin(\omega_1 t) \quad (3)$$

From equations (1) - (3) when defined as

$$Z_1 = \sqrt{\frac{L_r}{C_r}} \quad \text{and} \quad \omega_1 = \frac{1}{\sqrt{L_r C_r}} \quad (4)$$

Similarly, at $t = t_1$, the current flowing through I_{Df} decreases to zero and the current flowing through I_n increases by equal to the input current. Therefore, S_n will turn on with zero-current switching because L_r is connected in series and D_f will turn off with zero-current switching [18].

Figure 3 (b) Stage 2: $t_1 < t < t_2$. In this initial state, time $t = t_1$ yields characteristics $I_b = 0$, $I_{Lr} = I_n = I_L$, $I_{Df} = 0$, $V_{Csb} = V_{Cr} = V_o$, and $V_{Cr} = V_{Ca}$. Similarly, in this initial state, the D_f is turned off, Thus the differentiation of resonances through $C_{sb}-D_a-S_n-L_r-C_r$ and $C_a-S_b-L_r-C_r$. The energies of the C_{sb} and C_a capacitors are transferred to L_r and C_r . $I_{Lr}(t)$ and $V_{Ca}(t)$ can be expressed as follows:

$$I_{Lr}(t) = I_L - \frac{V_{Ca} - V_o}{\omega_2 L_r} \sin(\omega_2 t) \quad (5)$$

$$V_{Cr}(t) = V_{Csb}(t) = -(V_{Ca} - V_o) \cos(\omega_2 t) + V_{Ca} \quad (6)$$

From Equation (5) and Equation (6), when

$$\omega_2 = \frac{1}{\sqrt{L_r (C_a + C_{sb})}} \quad (7)$$

Similarly, at $t = t_2$, D_r starts (turns on) with zero-voltage switching as soon as the C_r capacitor voltage is $V_{Cr} = V_L$; thus, this state ends. However, C_{sb} and C_a discharges are equal to V_{Ca} until the end state and the current of the resonant inductor is equal to I_{Lr} . The resonances beginning in the previous stage continue through $C_{sb}-D_a-S_n-L_r-D_r-V_L$ and $C_a-S_b-L_r-D_r-V_L$. The current I_{Lr} increased, whereas V_{Csb} and V_{Cr} decreased. The current I_{Lr} has its maximum value $I_{Lr} = I_{Lrmax}$ when V_{Csb} and V_{Cr} are equal to V_L , after which the current of the resonant inductor is equal to the maximum value, and because of the negative voltage generated between the terminals of L_r , I_{Lr} begins to decrease continuously [19]-[20]. Similarly, voltages V_{Csb} and V_{Cr} were also reduced. $I_{Lr}(t)$ and $V_{Cr}(t)$ can be expressed as follows:

$$I_{Lr}(t) = \frac{V_o - V_i}{Z_3} \sin(\omega_3 t) + I_{Lr} \quad (8)$$

$$V_{Ca}(t) = V_{Csb}(t) = (V_o - V_i) \cos(\omega_3 t) + V_i \quad (9)$$

The duration of this period was determined using the following equation (10)

$$t_{23} = \frac{1}{\omega_3} \cos^{-1} \left(\frac{-V_i}{V_o - V_1} \right) \quad (10)$$

Therefore, Z_3 and ω_3 were obtained from the equation (11) and equation (12)

$$Z_3 = \sqrt{\frac{L_r}{C_{ra} + C_{sb}}} \quad (11)$$

$$\omega_3 = \frac{1}{\sqrt{L_r (C_{ra} + C_{sb})}} \quad (12)$$

At $t = t_3$, V_{Csb} and V_{Ca} are zero. Similarly, the ILr current is greater than the input current, and V_{Csb} and V_{Ca} are equal to zero ($V_{Csb} = V_{Ca} = 0$). However, the residual current of the input current L_r begins to flow through the antiparallel diode S_b , where this state is complete.

Figure 3 (d) Stage 4 ($t_3 < t < t_4$) begins at $t = t_3$, $I_{sb} = (I_L - I_{Lr})$, $I_{Lr} = I_{sn} = I_{Lr}$, $I_{Df} = 0$, $V_{Csb} = V_{Cr} = 0$, and $V_{Cr} = V_i$. This state begins when the antiparallel diode of Sb is turned on and I_{Lr} is reduced to a linear value until it drops to equal I_L . However, to operate the soft switch for the primary switch, PWM signal control must be implemented while the parallel protection diode of Sb is in the turn-on state. Similarly, during this period, the PWM signal control is directed to control the boost switch while the boost switch voltage is zero. Therefore, S_b was completely turned on with a zero-voltage transition. However, the state in which the Sb antiparallel diode is in the turn-on state is called a zero-voltage transition. The $I_{Lr}(t)$ can be expressed as (13) and (14)

$$t_{34} = \frac{I_{Lr}}{V_i} L_r \quad (13)$$

$$I_{Lr}(t) = \frac{V_i}{L_r} t + I_{Lr} \quad (14)$$

Similarly, at $t = t_4$, this state is completed when the current of the resonant inductor decreases to equal I_L .

Figure 3 (e) Stage 5: ($t_4 < t < t_5$) The start time of this state is $t = t_4$, $I_b = 0$, $I_{Lr} = I_b = I_L$, $I_{Df} = 0$, $V_{Cb} = V_{Ca} = 0$ and $V_{Cr} = V_i$. However, at $t = t_4$, I_b increases and varies with the input current, and the current of I_{Lr} decreases to zero. Similarly, $I_{Lr}(t)$ can be expressed as (15) and (16)

$$t_{45} = \frac{I_L}{V_i} L_r \quad (15)$$

$$I_{Lr}(t) = -\frac{V_i}{L_t} t + I_L \quad (16)$$

Similarly, $t = t_5$, the state of $I_b = I_i (I_L)$, and $I_{Lr} = 0$, which is the D_a and D_r turn-off period with zero-current switching, thus completing this state.

Figure 3 (f) Stage 6: ($t_5 < t < t_6$) The beginning of this state is $t = t_5$, $I_b = I_L$, $I_{Lr} = I_n = 0$, $I_{Df} = 0$, $V_{C_r} = V_{C_a} = 0$ and $V_{C_r} = V_i$. This state is initiated when the current of I_{Lr} is zero and the current of I_b is equal to the input current [21]. Similarly, the boost switch turns on the input current and the resonant inductor is initiated between C_r , L_r , and C_a . Thus, the energy of C_r is transferred to L_r and C_a through antiparallel diode S_n . In this case, the V_{C_r} voltage continued to decrease until it was restarted. Similarly, as V_{C_a} increased, I_{Lr} increased.

The I_{Lr} current in the reverse direction causes V_{C_r} and V_{C_a} to remain constant. During this period, the I_{Lr} continued to decrease. The snubber switch-control PWM signal S_n is removed during this period, when the antiparallel diode of S_n is in the turn-on state. Therefore, S_n was completely turned off with a zero-voltage transition [22]. The $V_{C_r}(t)$ and $V_{C_a}(t)$ resonant capacitors can be expressed as (17) and (18)

$$V_{C_r}(t) = \frac{V_i C_x}{C_r} + \frac{V_i C_x}{C_a} \cos(\omega_x t) \quad (17)$$

$$V_{C_a}(t) = \frac{V_i C_x}{C_a} + \frac{V_i C_x}{C_r} \cos(\omega_x t) \quad (18)$$

From Equation (17) and Equation (18), when C_x and ω_x are equation (19) and (20)

$$C_x = \frac{C_r C_a}{C_r + C_a} \quad (19)$$

$$\omega_x = \frac{1}{\sqrt{L_r C_x}} \quad (20)$$

Similarly, this state is complete if $t = t_6$, because the energy of C_r begins to be transferred to C_a .

Figure 3 (g) Stage 7: ($t_6 > t > t_7$) This is the turn-on state of a typical boost converter. During this stage, the snubber circuit does not operate and S_b continues to turn on, which is equal to the input current. At $t = t_7$, the control PWM signal of S_b is removed and the procedure is complete.

Fig. 3 (h) Stage 8: ($t_7 < t < t_8$) In this initial state, $I_b = I_L$, $I_{Lr} = I_n = 0$, $I_{Df} = 0$, $V_{C_b} = 0$, $V_{C_a} = V_i$ and $V_{C_r} = 0$. C_b is then charged, causing V_{C_a} to peak under a constant input current. In this case, the voltage rise is limited by C_b , thus causing S_b to switch to zero voltage [23]. Therefore, the $V_{C_a}(t)$ snubber circuit can be expressed as (21) and (22)

$$t_{78} = \frac{V_i}{I_i} C_s \quad (21)$$

$$V_{cb}(t) = \frac{I_L}{C_b} t \quad (22)$$

Similarly, at $t = t_8$, the voltage of C_b is equal to that of C_a ($V_{cb} = V_{ca} = V_i$), D_a turns off under zero-voltage switching, and this state is completed. However, when D_a was turned on with zero-voltage switching, the voltage of C_b was equal to that of C_a [24]. Similarly, both C_b and C_a charge linearly under a constant input current, and $V_{ca}(t)$ resonant capacitor can be represented as follows:

$$V_{ca}(t) = V_{cb}(t) = \frac{I_L}{C_a + C_b} t \quad (23)$$

the time of this interval is

$$t_{89} = \frac{V_o}{I_L} (C_a + C_b) \quad (24)$$

However, at $t = t_9$, the voltages of C_b and C_a are equal to $V_{cb} = V_{ca} = V_o$; at the same time, D_f will turn on with zero-voltage switching, and D_a will turn off with zero-voltage switching; this state is completed.

Figure 3 (j) Stage 10: ($t_9 < t < t_{10}$) This state is $I_b = 0$, $I_n = 0$, $I_{Df} = I_L$, $V_{cb} = V_{ca} = V_o$, and $V_{cr} = V_i$. This state begins when D_f is switched on under zero voltage switching. In this state, power from the input and main inductors is transferred to the output, where the load is relayed in the circuit. However, at the end of this state, the transition period is complete and returns to its initial state condition.

3.2. Design Principles

This section describes the design principle of the zero-voltage boost converter with a circuit. The snubber in this research is divided into two components: a boost converter design part and a snubber circuit design part, which contain the evaluation parameters listed in Table 1.

However, for this evaluation, the configuration duty cycle (D) = 70%, the estimated efficiency (η) = 95%, the estimated ripple input (ΔI_L) = 20%, and the approximate input power (P_i) = 640 W, so the maximum value of the input current (I_{imax}) is

$$I_{imax} = 1.15 \left(\frac{P_i}{V_i} \right) = 1.15 \left(\frac{640}{100} \right) = 7.37 A$$

Similarly, once the maximum input current is determined, the snubber inductor can be selected as

$$L_r = \frac{V_o}{I_{i\max}} 3t_{rr} = \frac{300}{7.37} \times 55 \times 10^{-9} \geq 2.24 \mu\text{H}$$

This design required a snubber circuit switch device to support high currents of up to $3I_{i\max}$. Therefore, the capacitance of C_r must not exceed 10 nF.

The proposed boost converter uses a PWM signal to control the boost switch when the boost switch has zero voltage and S_b current is negative. Therefore, the boost switch operates under zero-voltage transition. Similarly, a zero-voltage transition period occurs when the S_b current is negative, as described in Stage 4.

Table 1.
Parameters of the design and evaluation of the mechanism.

Parameter	Symbol	Value
Output voltage	V_o	300 V
Input voltage	V_i	100 V
Output power	P_o	500 W
Switching frequency	f_s	100 kHz
Main inductance	L_f	450 μH
Output capacitor	C_f	300 μF
Resonance inductance	L_r	4.5 μH
Resonance capacitor 1	C_r	10 nF
Resonance capacitor 2	C_a	10 nF
Snubber capacitor	C_s	3.5 nF
Boost diode	D_f	80 A/600 V/ $t_{rr} = 55 \times 10^9$
Snubber diode 1	D_r	80 A/600 V/ $t_{rr} = 55 \times 10^9$
Snubber diode 2	D_a	80 A/600 V/ $t_{rr} = 55 \times 10^9$

However, the minimum zero-voltage transition period was calculated as 548 ns. As shown in Figure 4 (b), the zero-voltage change depends on the time and value of C_r and C_a capacitors. Therefore, the values of C_r and C_a capacitors used must not exceed 10 nF.

In the design of the L_r inductor and C_a capacitor, the optimal value of the L_r inductor is 6 μH and the value of the C_a capacitor is 10 nF. If the design is designed to increase the value, the duration of the zero-voltage and zero-current transitions will increase, which causes a loss of renewable energy. Thus, the loss in the entire system increases, and the efficiency decreases. Similarly, this boost converter offers a C_s capacitor, that is, the capacitor of the snubber circuit, and the turn-off time of the boost switch should be greater than the zero-voltage transition. Therefore, the value of capacitor C_s is defined as 3.3 nF.

4. Results and Discussion

This topic involves conducting experiments on the designed and constructed mechanisms. However, during the evaluation, we simulated the results using the MATLAB/Simulink program and compared them with the actual measurements taken from the created mechanisms. Our assessment focused on the initial power loss and performance of the boost converter circuit, with specific attention paid to evaluating the effectiveness of the zero-voltage switch. Additionally, we evaluated the performance of both non-sububber and snubber excitation circuits in the second part of our evaluation. Nevertheless, the MATLAB/Simulink program offers a user-friendly simulation schematic that provides accurate results. This is illustrated in Fig. 4.

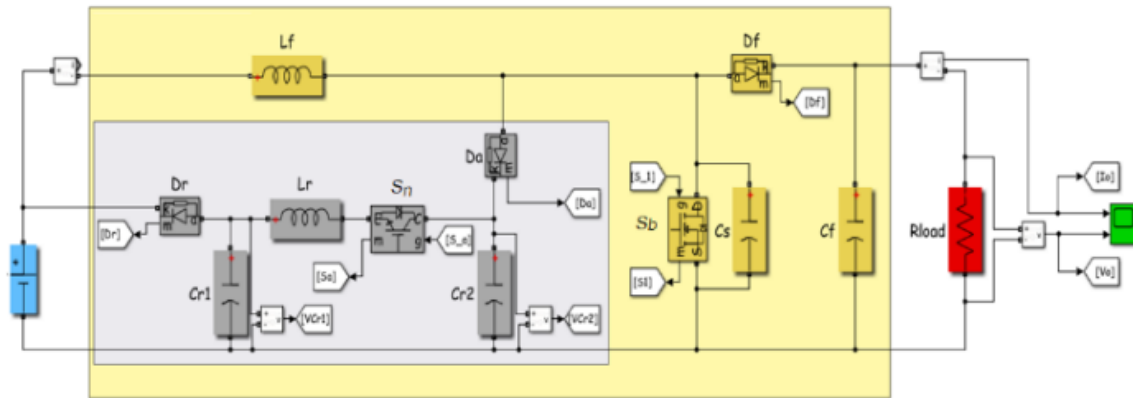


Figure 4.
Schematic of the simulation implemented in MATLAB/Simulink.

The analysis involved investigating the behavior of the device within the circuit. The main waveform related to the zero-voltage switch operation of the boost converter is measured when the snubber is activated. The measured waveform was then compared to the waveform generated using the MATLAB/Simulink simulation, as shown in Fig. 5.



Figure 5.
Experiments on boost converter and snubber.

As shown in Figures 6 (a) and (b), the operation occurred during the time interval $t_o < t < t_i$. During this time, S_b and S_n were in the turn-off state, allowing the input current to flow through diode D_f . This turning off of the boost converter circuit occurs before $t = t_o$, and the specific parameters are set as $t = t_o$, $I_b = 0$, $ID_f = I_r$, $I_{Lr} = I_n = 0$, $V_{Ca} = V_o$, and $V_{Cr} = 0$. As switch S_n

turns on at $t = t_0$ with a certain ratio of the PWM waveform, D_a is enabled under zero-current switching conditions. This led to an increase in the current of S_n and a decrease in ID_f . Simultaneously, C_r was also charged. Similarly, at $t = t_1$, ID_f decreases to zero and the current of S_n approaches the input current. Simultaneously, C_r is charged to a certain V_{ca} . This implies that S_n operates under zero-current switching conditions because the series L_r and D_f are turned off.

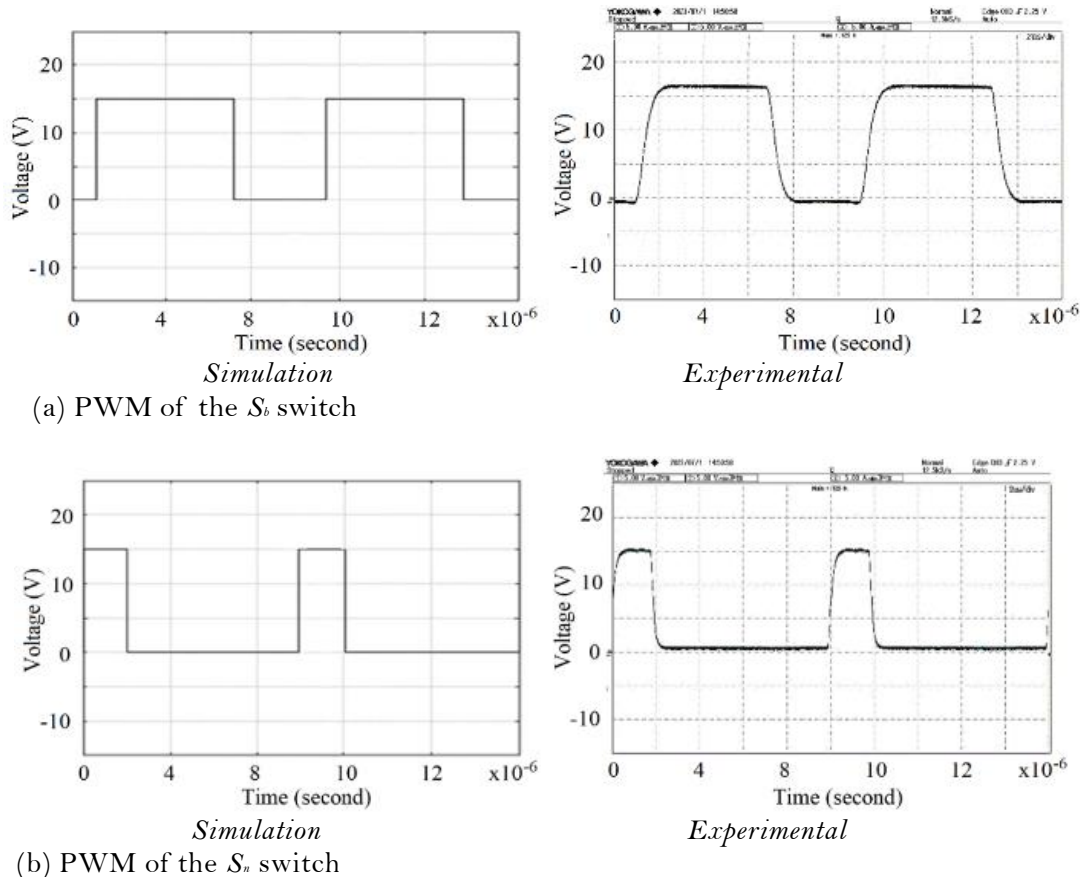


Figure 6. Simulation and experimental results of the switch operation.

Figure 6 (a) and (b) show the design and evaluation of a zero-voltage boost converter with a snubber circuit that uses a TMS320F28377S microcontroller to control the switching of power electronics. It was found that the mechanism can be operated for its intended purpose. Similarly, using a TMS320F28377S microcontroller simulating the switching of a device in the environment of a MATLAB/Simulink program, the switching behavior of the boost converter can be objectively studied and the theoretical accuracy described can be confirmed.

Figure 7. When $T_1 < T < T_2$, the initial state is $T = T_1$, and the characteristics of the voltage and current in different devices are $I_b = 0$, $I_{Lr} = I_n = I_L$, $ID_f = 0$, $V_{Cb} = V_{Cr} = V_o$, and $V_{Cr} = V_{Ca}$. However, once the diode (D_f) turns off, two distinct resonance characteristics are observed in the configurations of $C_{st}-D_a-S_n-L_r-C_r$ and $C_a-S_b-L_r-C_r$. The energy stored in the C_s and C_r capacitors is then transferred to L_r and C_r . When $t = t_2$, the snubber diode D_r is activated using zero-voltage switching conditions as soon as the capacitor voltage C_r matches the input voltage. At this

point, the C_a and C_r capacitors discharge from the V_{ca} voltage and reach the end of their discharge cycle.

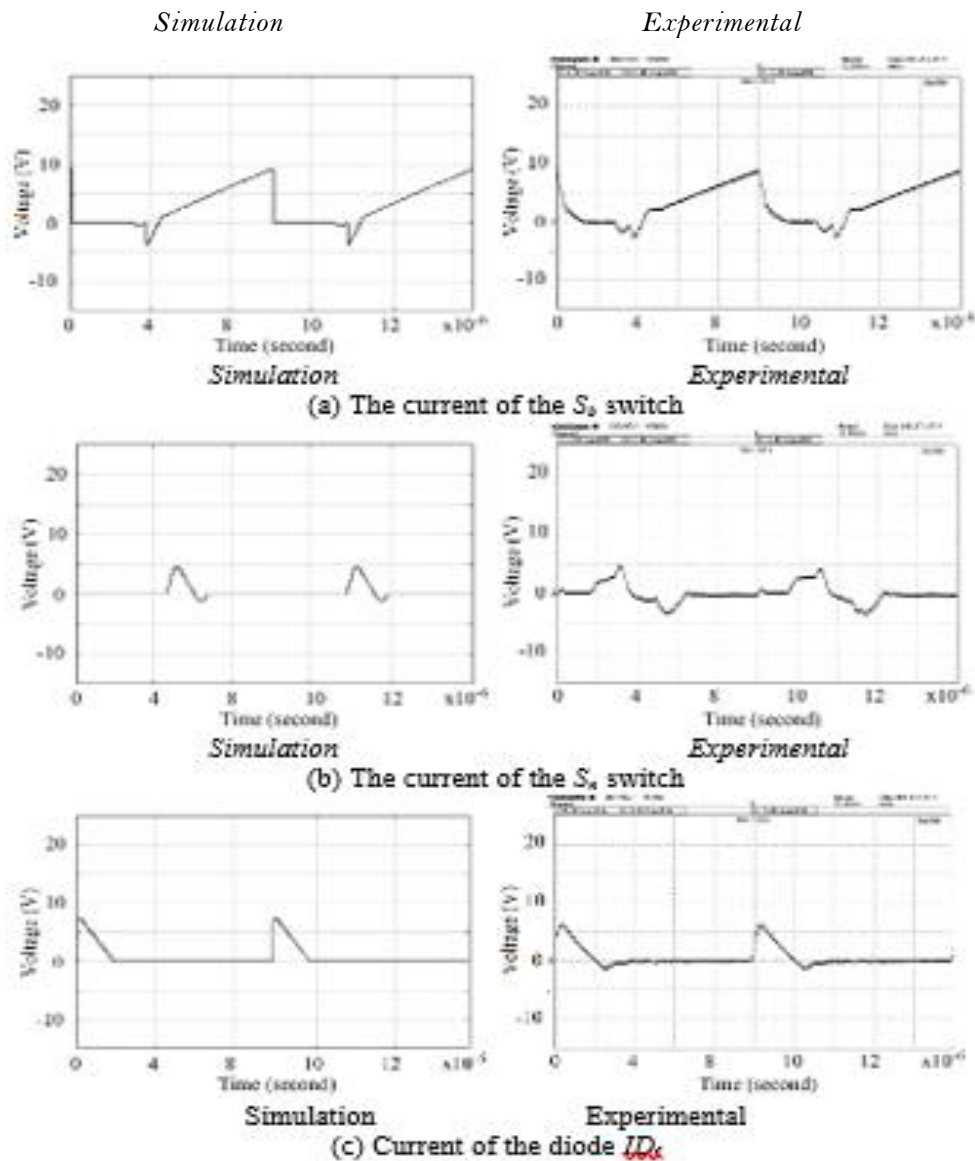


Figure 7.
Simulation and experimental results of the device.

The above experiments can determine whether the mechanism can work as intended, and from the simulation, the switching behavior of boost and snubber converters can be studied.

Figure 8 (a) and (b) show that the above experiments can be used to determine whether the mechanism can work as intended, and the switching behavior of the snubber can be studied. When the condition begins at time $t = t_s$, the device in the circuit will have a current and voltage represented by $I_s = 0$, $I_L = I_m$, $I_D = 0$, $V_C = V_C = V_{ca}$ and $V_r = V_i$. Stage 2 resonance continued through the C_r - D_r - S_1 - L_r - D_1 - V_i

and C_r - S_b - L_r - D_r - V_i pathways. During this process, the current of the L_r inductor increases, whereas the voltages V_{cs} and V_{cr} decrease.

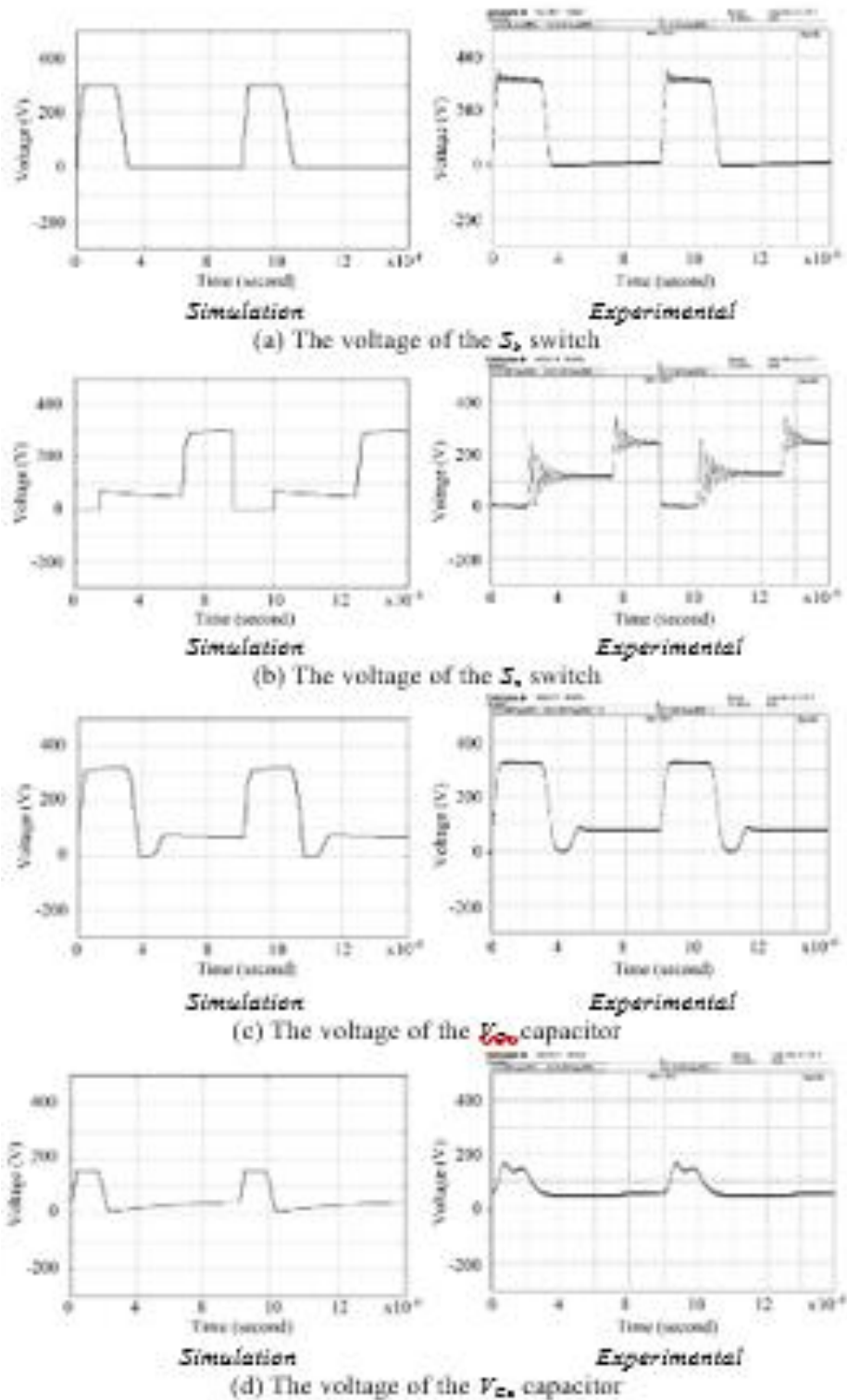


Figure 8.

Snubber switch simulation and experimental results.

Once the current in the inductor reaches its maximum, I_{Lr} starts to decrease owing to the negative pressure at the terminals of the L_r inductor. Consequently, voltages V_{cs} and V_{cr} also decrease synchronously. Nevertheless, in the subsequent section, a prototype mechanism trial was devised to juxtapose the performance traits of two distinct categories: one incorporating a zero-voltage switch, and the other devoid of such a switch. The device parameters for this evaluation are listed in Table 1, which has already been described above.

Based on the specifications listed in Table 1, the tests included an input voltage of 100 volts and an output voltage of 300 volts. The switch frequency used in this experiment was 100 kHz. This mechanism could supply power to a load of 500 W. This experimental procedure examines the input and output currents of a specially designed mechanism to evaluate the relationship between the input and output powers as well as the overall performance. As shown in Table 2, the results of the experiments clearly demonstrate that the zero-voltage switches exhibit a significantly superior performance.

Table 2.

Performance comparison of the two switch characteristics.

Status ZVS	V_{in} (V)	I_{in} (A)	P_{in} (W)	V_{out} (V)	I_{out} (A)	P_{out} (W)	η (%)
Operate	100	6.4	640	315	1.73	545	85.16
Non operate	100	6.8	680	307	1.76	540	78.41

To validate the experiment, the prototype mechanism was compared with a simulation. The results obtained from the analysis of Fig. 9 (a) and (b) indicate that the operation of the S_b switch under zero-voltage switching conditions introduces new intervals for voltage and current switching, resulting in the smooth operation of the switch. This significantly reduces the stress on the switch device and minimizes electromagnetic interference (EMI). These findings are considered satisfactory. However, it is important to note that achieving a complete soft switch requires an appropriate design of the inductor, capacitor, and PCB layouts tailored to a specific application.

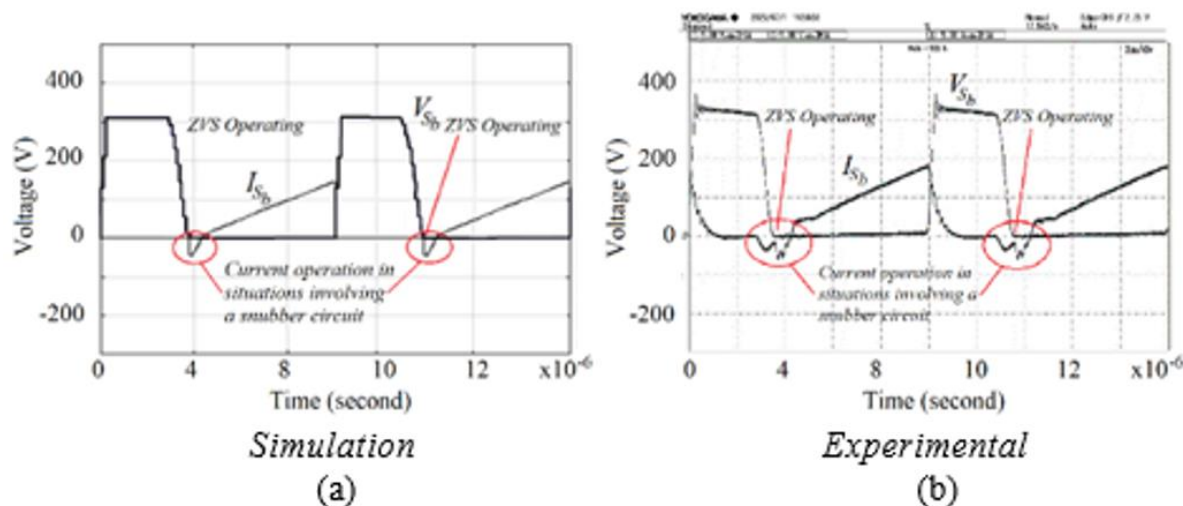


Figure 9.

The operating state of the zero-voltage switch master mechanism with snubber.

Figure 9. (a) and (b) Analysis of current operation under conditions with a snubber circuit, referring to the functioning of an electrical system that includes the use of a snubber circuit. A snubber circuit is a protection mechanism that is connected in parallel with a load or switch, and helps control and manage the voltage or current in the circuit. In this context, the current operation under conditions with a snubber circuit involves the flow of electrical current through the circuit while the snubber circuit is actively functioning. The snubber circuit is designed to absorb and dissipate excess energy or voltage spikes that may occur in the circuit, thereby protecting sensitive components from damage. During current operation, the snubber circuit operates in conjunction with a load or switch, allowing the electrical current to flow through the circuit while regulating and protecting against sudden surges or fluctuations in voltage. This ensures the smooth and efficient operation of the electrical system while minimizing the risk of damage to components or equipment. Overall, current operation under conditions with a snubber circuit involves the safe and controlled flow of electrical current through the circuit, owing to the presence of a snubber circuit that helps protect against voltage spikes and fluctuations.

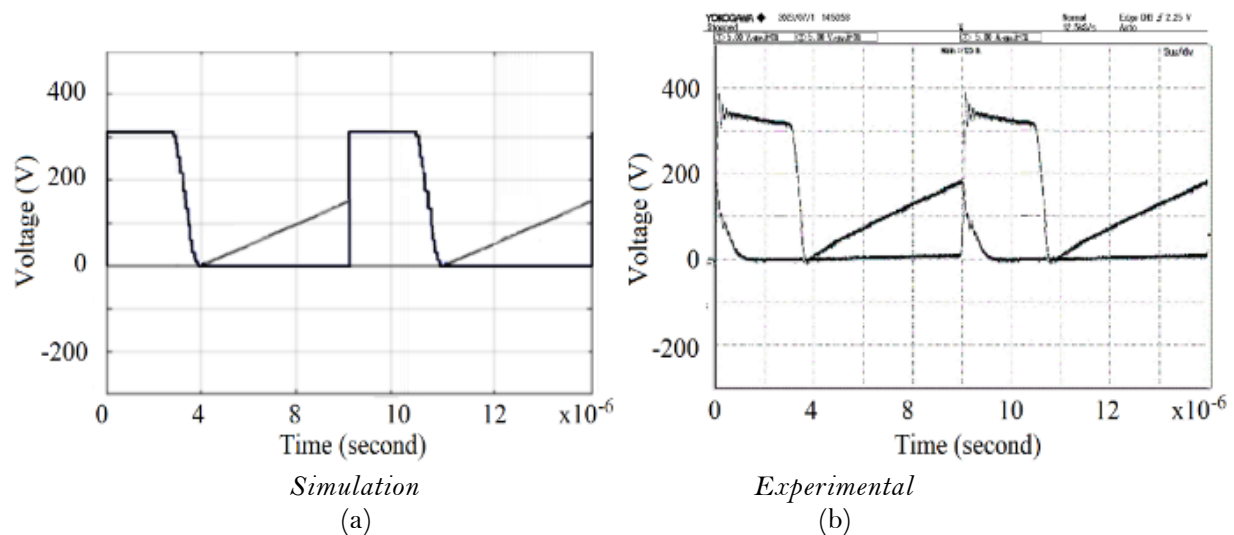


Figure 10.
The operating state of the no-switch conditions master mechanism.

Similarly, the results of the experiments conducted under no-switch conditions at zero voltage are shown in Fig. 10 (a) and (b). However, it has been discovered that abruptly turning off the switch during periods and high-frequency ranges can trigger activation of the S_1 switch. This can lead to elevated stress levels, increased electromagnetic interference (EMI), and other effects. It should be noted that damage, particularly to the switching device, is a potential outcome in a circuit failure. However, comparing the experimental and simulation results can establish the accuracy of the research hypotheses set forth in the objectives.

However, after conducting experiments on the prototype mechanisms and comparing them with simulations, it is evident that there is a certain level of consistency that affirms their principled validity and reliability. Furthermore, it is important to note that the performance of a mechanism varies with changes in input voltage. In the following section, we provide conclusions and recommendations for those interested in further advancing this topic.

5. Conclusion

This study introduces a technique called the zero-voltage switch for the boost converter mechanism. This technique involves the use of snubber band excitation through the microcontroller control

TMS320F2879D to generate the boost switch control signal (S_b) for the boost converter circuit. In addition, the contract circuit uses a snubber switch (S_n) in the snubber mechanism. However, the evaluation and experiments were conducted in accordance with three defined objectives. An analysis of the boost switch waveform shows that, during the turn-off phase, the current in the boost switch flows in the negative direction, whereas during the turn-on phase, the current flows in the positive direction when the voltage is zero, which follows the method described above. The experimental results were compared with simulations using the MATLAB/Simulink program, and the waveform characteristics were found to be consistent. By incorporating snubber excitation, it was observed that the efficiency of the boost circuit can be increased to 85.16%, which is 6.75% greater than that without a zero-voltage switch. If the simulation evaluation results are considered and analyzed in comparison with the prototype mechanism, the results are similar. However, the simulation using MATLAB/Simulink is a mathematical simulation that does not have any dynamic effects. Similarly, experiments with prototype mechanisms have many effects, such as duty cycle ratio, operating frequency adjustment, and equipment parameter tolerance. Furthermore, a boost converter circuit with snubber excitation can operate reliably even under voltage drop or overvoltage conditions because it eliminates stressful situations and prevents equipment breakdown caused by EMI losses.

Similarly, regarding recommendations and guidelines for enhancements, prospective individuals should carefully select and devise the most appropriate apparatus to ensure the long-lasting nature of the PCB and its mechanism, ultimately resulting in enhanced efficiency. However, one must also consider the character of the generation process of the digital control signal when determining the frequency of switches to effectively satisfy the required responsiveness.

Acknowledgment:

The researchers and working group express their gratitude to Dhonburi Rajabhat University, Thailand, for their support in providing laboratories and research instruments that allowed them to successfully achieve their objectives.

Copyright:

© 2024 by the authors. This article is an open access article distributed under the terms and conditions of the Creative Commons Attribution (CC BY) license (<https://creativecommons.org/licenses/by/4.0/>).

References

- [1] da Silva, Evandro Soares, et al. "An improved boost PWM soft-single-switched converter with low voltage and current stresses." *IEEE Transactions on Industrial Electronics* 48.6 (2001): 1174-1179.
- [2] Li, Wuhua, et al. "Interleaved converter with voltage multiplier cell for high step-up and high-efficiency conversion." *IEEE transactions on power electronics* 25.9 (2010): 2397-2408.
- [3] Mohammadsalehian, Shamim, et al. "An Improved Buck Converter with Zero Output Current Ripple and Soft-Switching Capability." 2021 IEEE Industry Applications Society Annual Meeting (IAS). IEEE, 2021.
- [4] Choi, H-C., and H-B. Shin. "A new soft-switched PWM boost converter with a lossless auxiliary circuit." *International Journal of Electronics* 93.12 (2006): 805-817.
- [5] Wu, Chao-Cheng, and Chung-Ming Young. "New ZVT-PWM DC/DC converters using active snubber." *IEEE Transactions on Aerospace and Electronic Systems* 39.1 (2003): 164-175.
- [6] Ting, Naim Suleyman, Fulya Aslay, and Yakup Sahin. "A novel zero voltage transition boost converter and artificial neural network-based estimation of converter efficiency." *International Journal of Circuit Theory and Applications* 50.9 (2022): 3251-3265.
- [7] Banik, Samudra Prosad, and Debasis Bagchi, eds. *Biofuels: Scientific Explorations and Technologies for a Sustainable Environment*. CRC Press, 2024.
- [8] Rao, Burle Tulasi, and Dipankar De. "Effective leakage energy recycling in high gain DC-DC converter with coupled inductor." *IEEE Transactions on Circuits and Systems II: Express Briefs* 69.7 (2022): 3284-3288.
- [9] Chen, Keming, and Tomas A. Stuart. "A study of IGBT turn-off behavior and switching losses for zero-voltage and zero-current switching." [Proceedings] *APEC'92 Seventh Annual Applied Power Electronics Conference and Exposition*. IEEE, 1992.

- [10] Chen, Keming, and Tomas A. Stuart. "A study of IGBT turn-off behavior and switching losses for zero-voltage and zero current switching." [Proceedings] APEC'92 Seventh Annual Applied Power Electronics Conference and Exposition. IEEE, 1992.
- [11] Ogunseye, A. A., et al. "A new Inductorless single capacitor step down DC-to-DC converter design." *Scientific African* 19 (2023): e01572.
- [12] Lin, B-R., J-J. Chen, and F-Y. Hsieh. "Analysis and implementation of a bidirectional converter with high conversion ratio." 2008 IEEE International Conference on Industrial Technology. IEEE, 2008.
- [13] Das, Pritam, and Gerry Moschopoulos. "A comparative study of zero-current-transition PWM converters." *IEEE Transactions on Industrial Electronics* 54.3 (2007): 1319-1328.
- [14] Bose, Bimal K. "Power electronics-a technology review." *Proceedings of the IEEE* 80.8 (1992): 1303-1334.
- [15] Pattnaik, Swapnajit, Anup Kumar Panda, and Kamalakanta Mahapatra. "Efficiency improvement of synchronous buck converter by passive auxiliary circuit." *IEEE Transactions on Industry Applications* 46.6 (2010): 2511-2517.
- [16] Miryala, Vamshi Krishna, et al. "Layout inductance assisted novel turn-on switching loss recovery technique for SiC MOSFETs." *IEEE Journal of Emerging and Selected Topics in Industrial Electronics* 2.4 (2021): 513-525.
- [17] Alavi, Peyman, et al. "New auxiliary circuit for boost converter to achieve soft-switching operation and zero input current ripple." *IET Power Electronics* 13.17 (2020): 3910-3921.
- [18] Chen, Yie-Tone, and Sheng-Zhi Mo. "A bridgeless active-clamp power factor correction isolated SEPIC converter with mixed DCM/CCM operation." 2013 1st International Future Energy Electronics Conference (IFEEEC). IEEE, 2013.
- [19] Ting, Naim Suleyman, Ismail Aksoy, and Yakup Sahin. "ZVT-PWM DC-DC boost converter with active snubber cell." *IET Power Electronics* 10.2 (2017): 251-260.
- [20] Wu, Hongfei, et al. "Fixed-frequency PWM-controlled bidirectional current-fed soft-switching series-resonant converter for energy storage applications." *IEEE Transactions on Industrial Electronics* 64.8 (2017): 6190-6201.
- [21] Ye, Xiaohui, et al. "Study on Initialization Strategy of LCC-HVDC System." 2020 IEEE International Conference on High Voltage Engineering and Application (ICHVE). IEEE, 2020.
- [22] Li, Wuhua, et al. "General derivation law of nonisolated high-step-up interleaved converters with built-in transformer." *IEEE Transactions on Industrial Electronics* 59.3 (2011): 1650-1661.
- [23] Belu, Radian. *Energy storage, grid integration, energy economics, and the environment*. CRC Press, 2019.
- [24] Hwu, K. I., Y. T. Yau, and W. Z. Jiang. "Soft switching converter with output voltage ripple minimized." *International Review of Electrical Engineering* 12.3 (2017): 183-194.